

A Comparison of Stealthy Sensor Attacks on Control Systems

Navid Hashemi¹, Carlos Murguia², and Justin Ruths¹

Abstract—As more attention is paid to security in the context of control systems and as attacks occur to real control systems throughout the world, it has become clear that some of the most nefarious attacks are those that evade detection. The term *stealthy* has come to encompass a variety of techniques that attackers can employ to avoid detection. Here we show how the states of the system (in particular, the reachable set corresponding to the attack) can be manipulated under two important types of stealthy attacks. We employ the chi-squared fault detection method and demonstrate how this imposes a constraint on the attack sequence either to generate no alarms (zero-alarm attack) or to generate alarms at a rate indistinguishable from normal operation (hidden attack).

I. INTRODUCTION

For many decades, Control Theory operated in a challenging but happy place in which problems pitted designers against the world, a haphazard place of disturbances and uncertainty. The past decade has seen the rise in concern over attacks on control systems, which necessarily requires us to shift our focus to a problem of designer against attacker, a strategic and knowledgeable entity that seeks to exploit the weaknesses of our systems and control frameworks.

Control systems have become an attractive target to attackers due to accessibility, impact, and obfuscation. Large-scale control systems such as process control plants are increasingly moving toward Ethernet-like technology to communicate data throughout the system. This new architecture provides new capabilities but also opens systems up to the same types of cyber attacks that banking and database companies endure. These systems also represent major industry or municipal infrastructure, which means damaging them makes large impact. Finally, these systems are large and complex enough - and often not monitored well enough - for attackers to manipulate the system without being detected.

The literature of attack detection has concerned itself with designing methods to effectively monitor systems and detect anomalies [1]–[6]. The origin of many of these methods arise from fault detection, but have been retooled to consider antagonistic and strategic “faults”. A key component of this body of work is to understand the limits of these detectors, and identifying attacks that are stealthy to these methods is a critical way to benchmark detector performance. The

term *stealthy* has taken on several meanings in the literature. It has been used to address attacks that do not induce the detectors to raise alarms; we rename these *zero-alarm attacks* to be more precise [1], [7], [8]. It has also referred to an attack that changes the alarm rate of the detector by only a small amount; we call these *perturbation attacks* [9], [10]. We define a *hidden attack* which exactly mimics the alarm rate of the detector. Stealthy is also used to describe attacks that effect the uncontrollable and unobservable modes of the system and, therefore, do not propagate to any measurement or estimated state of the system [2]. Replay attacks also fall into the category of stealthy attacks as they replay past (recorded) data back to the monitoring equipment [11].

The attacks on unobservable/uncontrollable modes and replay attacks completely circumvent the detectors, which is interesting and relevant to the broader context of security, but requires a countering strategy that goes beyond detectors. The perturbation attack has a relatively small effect on the system compared with zero-alarm and hidden attacks, thus we also omit it from this study.

We use this manuscript to present a distribution-based perspective on attack detection. As part of this we present a equitable comparison between the impact of zero-alarm and hidden attacks. We use the set of states reachable by the system when driven by the attacker input as a metric for this comparison. To achieve this, we present several novel results to formulate and to find ellipsoidal outer bounds on the reachable sets of the system corresponding to attacks.

II. BACKGROUND

In this work, we study stochastic discrete-time linear time-invariant (LTI) systems

$$\begin{cases} x_{k+1} = Fx_k + Gu_k + v_k, \\ y_k = Cx_k + \eta_k, \end{cases} \quad (1)$$

in which the state $x_k \in \mathbb{R}^n$, $k \in \mathbb{N}$, evolves due to the state update provided by the state matrix $F \in \mathbb{R}^{n \times n}$, the control input $u_k \in \mathbb{R}^m$ filtered by the input matrix $G \in \mathbb{R}^{n \times m}$, and the i.i.d. zero-mean Gaussian system noise v_k with covariance matrix R_1 . The output $y_k \in \mathbb{R}^p$ aggregates a linear combination, given by the observation matrix $C \in \mathbb{R}^{p \times n}$, of the states and zero-mean Gaussian measurement noise with covariance matrix R_2 . We assume that the pair (F, C) is detectable and (F, G) is stabilizable.

We consider the scenario that the actual measurement y_k can be corrupted by an additive attack, $\delta_k \in \mathbb{R}^p$. At some point in the process of measuring and transmitting the output to the controller the attacked output becomes

$$\bar{y}_k = y_k + \delta_k = Cx_k + \eta_k + \delta_k. \quad (2)$$

*This work was partially supported by the National Research Foundation (NRF), Prime Minister’s Office, Singapore, under its National Cybersecurity R&D Program (Award No. NRF2014NCR-NCR001-40) and administered by the National Cybersecurity R&D Directorate.

¹These authors are with the Departments of Mechanical and Systems Engineering at the University of Texas at Dallas, Richardson, Texas, USA. Navid.Hashemi, j.ruths@utdallas.edu

²C. Murguia is with the iTrust Centre at the Singapore University of Technology and Design, Singapore murguia.rendon@sutd.edu.sg

If the attacker has access to the measurements, then it is possible for the attack δ_k to cancel some or all of the original measurement y_k - so an additive attack can achieve arbitrary control over the “effective” output of the system.

As our approach leverages a fault-detection approach, we require an estimator to produce a prediction of the system behavior. In this work we use the steady state Kalman filter

$$\hat{x}_{k+1} = F\hat{x}_k + Gu_k + L(\bar{y}_k - C\hat{x}_k), \quad (3)$$

where $\hat{x}_k \in \mathbb{R}^n$ is the estimated state. The observer gain L is designed to minimize the steady state covariance matrix $P := \lim_{k \rightarrow \infty} P_k := E[e_k e_k^T]$ in the absence of attacks, where $e_k := x_k - \hat{x}_k$ denotes the estimation error. Existence of P is guaranteed since the pair (F, C) is assumed to be detectable [12]. Next, we define the residual sequence r_k

$$r_k := \bar{y}_k - C\hat{x}_k, \quad (4)$$

the difference between what we actually receive (\bar{y}_k) and expect to receive ($C\hat{x}_k$), which evolves according to

$$\begin{cases} e_{k+1} = (F - LC)e_k - L\eta_k + v_k - L\delta_k, \\ r_k = Ce_k + \eta_k + \delta_k. \end{cases} \quad (5)$$

In the absence of attacks (i.e., $\delta_k = 0$), it is straightforward to show that the r_k random variable falls according to a zero mean Gaussian distribution with covariance [8]

$$\Sigma = E[r_k r_k^T] = CPC^T + R_2. \quad (6)$$

In this work, we consider only one detector, the popular chi-squared detector. Although other alternatives exist, the chi-squared is easily the dominant choice for most research and it also provides a transparent choice to highlight the key messages we wish to communicate in this work. Similar analysis can be done with these other detector choices using attacks derived in our other work [7], [8], [13]. In the case of the chi-squared detector, a quadratic distance measure z_k is created to be sensitive to changes in the variance of the distribution as well as the expected value,

$$z_k = r_k^T \Sigma^{-1} r_k. \quad (7)$$

Since $r_k \sim \mathcal{N}(0, \Sigma)$, the z_k random variable, as the sum of the squares of normally distributed random variables, falls according to the chi-square distribution. Since $r_k \in \mathbb{R}^p$, this chi-squared distribution has p degrees of freedom. The chi-squared detector is summarized as follows: for given a threshold $\alpha \in \mathbb{R}_{>0}$ and the distance measure $z_k = r_k^T \Sigma^{-1} r_k$

$$\begin{cases} z_k \leq \alpha & \longrightarrow \text{no alarm,} \\ z_k > \alpha & \longrightarrow \text{alarm: } k^* = k, \end{cases} \quad (8)$$

alarm time(s) k^* are produced. The Σ^{-1} factor in the definition of z_k rescales the distribution ($E[z_k] = p$, $E[z_k z_k^T] = 2p$) so that the threshold α can be designed independent of the specific statistics of the noises v_k and η_k ; instead, it can be selected simply based on the number of sensors, p .

It is important to note that because of the infinite support of noises v_k and η_k , the distance measure z_k , distributed

according to a chi-squared distribution, also has infinite support. Therefore, even in the absence of attacks, we expect that the detector will generate alarms because some values drawn from the distance measure distribution will exceed the threshold α . Such alarms in the absence of an attack are called *false alarms*. Because we can characterize the chi-squared distribution analytically, we have an exact relation between the choice of the threshold α and the expected rate of false alarms \mathcal{A} generated by the chi-squared detector.

Lemma 1: [8]. Assume that there are no attacks to the system and consider chi-squared detector, with threshold $\alpha \in \mathbb{R}_{>0}$, $r_k \sim \mathcal{N}(0, \Sigma)$. Let $\alpha = \alpha^* := 2P^{-1}(1 - \mathcal{A}^*, \frac{p}{2})$, where $P^{-1}(\cdot, \cdot)$ denotes the inverse regularized lower incomplete gamma function, then $\mathcal{A} = \mathcal{A}^*$.

A. Undetected Attacks

Some of the most insidious attacks on industrial control systems feature attack strategies that manipulate the system while all the time staying undetected. The effect of the attack can aggregate during this “stealthy” execution of the attack and the damage caused by the attack can spread. Past attacks on industrial control systems seem to favor these undetected attacks, such as the famous Stuxnet worm incident [14].

In many industrial settings fault detection is accomplished simply by assigning a collection of static rules (e.g., if a pressure in a vessel exceeds a given value). These offer little-to-no protection against stealthy adversarial attacks as the attack can deviate the actual system state while reporting a “spoofed” state that is within normal operating conditions. When detectors are implemented in control systems, these detectors limit what the attacker is able to accomplish if he/she seeks to remain undetected. We advance two notions of undetected attacks (we phrase these with respect to the chi-squared detector, however, the concept of these attack classes generalize to other detectors). These attack models require strong attacker knowledge and access, namely we assume that the attacker has perfect knowledge of the system dynamics, the Kalman filter, control inputs, measurements, and chi-squared procedure. In addition, the attacker has read and write access to all the sensors at each time step. The goal of these stealthy attacks is to construct a worst case scenario to bound the capabilities of attackers.

Zero-alarm attacks generate attack sequences that maintain the distance measure at or below the threshold, i.e., $z_k \leq \alpha$. These attacks generate no alarms during the attack. To satisfy this condition we define the attack as

$$\delta_k = -Ce_k - \eta_k + \Sigma^{\frac{1}{2}} \bar{\delta}_k, \quad (9)$$

where $\bar{\delta}_k \in \mathbb{R}^p$ is any vector such that $\bar{\delta}_k^T \bar{\delta}_k \leq \alpha$ and $\Sigma^{\frac{1}{2}}$ is the symmetric square root of Σ . This attack sequence leads the distance measure to become

$$z_k = (Ce_k + \eta_k + \delta_k)^T \Sigma^{-1} (Ce_k + \eta_k + \delta_k) \leq \alpha. \quad (10)$$

Since $z_k \leq \alpha$, no alarms are raised. A schematic of a zero-alarm attack is shown in Fig. 1. Although generating no alarms seems like a successful strategy to avoid detection, it is important to remember that in the attack-free case alarms

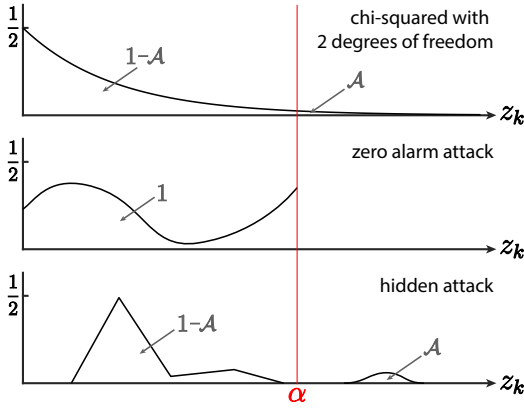


Fig. 1. The original (attack-free) z_k distribution (top) is chi-squared with p degrees of freedom (this paper uses examples in which $p = 2$). The threshold α is selected to satisfy a false alarm rate of \mathcal{A} , implying that in the attack-free distribution, the area under the distribution curve that falls beyond α is \mathcal{A} . In zero-alarm attacks (middle), $\bar{\delta}_k$ is selected such that z_k is no larger than α , implying that no alarms are raised under zero-alarm attacks. In hidden attacks (bottom), $\bar{\delta}_k$ is designed so that the fraction of the distribution that falls beyond α matches that of the attack-free distribution, which means that the alarm rate under the hidden attack is equal to the false alarm rate. The definition of the zero alarm and hidden attacks do not stipulate the shape of the density functions above and below α , although the allocation of mass in the density function greatly influences the effect of the attack on the reachable states.

are raised due to the infinite support of the distance measure distribution. Thus, before the attack, alarms are raised at a rate $\mathcal{A} > 0$ and after the attack the alarm rate becomes zero, $\mathcal{A} = 0$. While the detector does not monitor changes in the false alarm rate, it is possible that an operator might notice this discrepancy. This leads us to develop a second class of undetectable attacks. We are also motivated to develop the following attacks because they exploit the stochasticity to inject larger, more potent attacks.

Hidden attacks generate attack sequences that raise alarms at the same rate as the false alarm rate of the detector (i.e., alarms are raised at the same rate during the attack as are false alarms in the attack-free case). In hidden attacks, the attack sequence $\bar{\delta}_k$ in (9) is a random variable designed such that

$$\Pr(z_k > \alpha) = \Pr(\bar{\delta}_k^T \bar{\delta}_k > \alpha) = \mathcal{A}. \quad (11)$$

In other words, on average out of N time steps: $(1 - \mathcal{A})N$ time steps $\bar{\delta}_k^T \bar{\delta}_k \leq \alpha$ and the remaining $\mathcal{A}N$ time steps $\bar{\delta}_k^T \bar{\delta}_k > \alpha$. The chi-squared detector tuned to a false alarm rate \mathcal{A} effectively splits the z_k distribution into a part $z_k \leq \alpha$ and a part $z_k > \alpha$, where α is selected using Lemma 1. Hidden attacks ensure that the proportion of z_k values larger than α observed by the detector during the attack match the proportion expected in the attack-free case [15]. A schematic of a hidden attack is shown in Fig. 1.

B. Feedback

In order for the attack to propagate from the estimation error to the state, we need to incorporate a model of feedback in the control system. In this paper we assume static estimator feedback $u_k = K\hat{x}$. With this feedback the

closed-loop system becomes

$$\begin{cases} x_{k+1} = (F + GK)x_k + GK e_k + v_k, \\ e_{k+1} = (F - LC)e_k - L\delta_k - L\eta_k + v_k. \end{cases} \quad (12)$$

The estimation error updates according to, without attacks,

$$e_{k+1} = (F - LC)e_k - L\eta_k + v_k, \quad (13)$$

and with attacks of the form in (9),

$$e_{k+1} = Fe_k - L\Sigma^{\frac{1}{2}}\bar{\delta}_k + v_k. \quad (14)$$

Remark 1: Note that if the spectral radius $\rho[F] > 1$, then $\|E[e_k]\|$ (and also $\|E[x_k]\|$ due to the interconnection) diverges to infinity as k grows for any non-stabilizing k . That is, attacks of the form (9) may destabilize the system if $\rho[F] > 1$. If $\rho[F] \leq 1$, then $\|E[e_k]\|$ may or may not diverge to infinity depending on algebraic and geometric multiplicities of the eigenvalues on the unit circle. Thus we consider open-loop stable system matrices, $\rho[F] < 1$.

III. REACHABLE SET BOUNDS

In order to compare the effects of these different stealthy attacks, we require a metric to quantify the impact of each attack. A popular choice to quantify system impact due to a disturbance is the set of states reachable by the action of the disturbance. Here, we show two techniques to derive outer ellipsoidal bounds on the reachable states. The first, based on Linear Matrix Inequalities (LMIs), constructs a convex optimization problem, the solution of which is the ellipsoid that bounds the states driven by attacks. This approach provides more conservative estimates of the reachable set, but allows for the opportunity to simultaneously design system components, such as estimator and controller gain matrices, to reduce the size of the reachable set (see, e.g., [10], [15]). The second approach provides tighter bounds through the use of geometric ellipsoidal methods.

The different definitions of the zero alarm attack and the hidden attack naturally give rise to different reachable sets. The challenge of the hidden attack definition is that there are no constraints on the location of the \mathcal{A} mass that falls beyond α . This means that \mathcal{A} of the probability density function of the distance measure can be made arbitrarily large, which in turn makes the reachable sets driven by hidden attacks arbitrarily large. Therefore, it is not meaningful to define the outer bound of the reachable set corresponding to hidden attacks - it would simply be the entire state space. Instead, we introduce the notion of a \bar{p} -probable ellipsoid which encompasses the reachable set when the z_k distribution is truncated at \bar{z} , where $\Pr(z_k \leq \bar{z}) = \bar{p}$. This ellipsoid can be interpreted graphically as a level set of the distribution function of the reachable states (see Fig. 2). It is worth noting that the probability \bar{p} corresponds to the truncation of the z_k distribution and does not specify the probability that a point in the true reachable state set is in the \bar{p} -probable ellipsoid. While the later probability is closer to what we want to know, this would require knowing the complete distribution of reachable states which is what we aim to find in the first

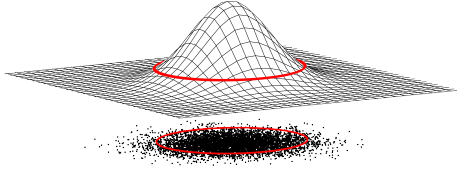


Fig. 2. The \bar{p} -probable ellipsoid captures a level set of the distribution of reachable states corresponding to when the system is driven by a truncated distance measure, such that $z_k \leq \bar{z}$, where $\Pr(z_k \leq \bar{z}) = \bar{p}$.

place. Notwithstanding, there is a one-to-one mapping from \bar{p} to level sets of the reachable set distribution, so increasing (resp., decreasing) \bar{p} necessarily expands (resp., shrinks) the ellipsoid level set, so this is not much of a restriction.

While we consider more general choices of \bar{p} in other work (see [15]), here we focus on the most immediate choice $\bar{p} = 1 - \mathcal{A}$ and so $\bar{z} = \alpha$. Recall that the hidden attack (see Fig. 1 and (11)) only requires the attacker to satisfy one statistic of the attack $\bar{\delta}_k$, namely $\Pr(z_k = \bar{\delta}_k^T \bar{\delta}_k \leq \alpha) = 1 - \mathcal{A}$. For a general hidden attack, we have no further information about the distribution of z_k (recall the shape of the distribution, beyond this one constraint, is completely free for the attacker to choose, see Fig. 1). Thus the only choice of \bar{p} that can be evaluated for a general hidden attack is $\bar{p} = 1 - \mathcal{A}$. This also simplifies the comparison of hidden attacks with zero alarm attacks. Selecting $\bar{z} = \alpha$ as the truncation point of the z_k distribution implies then that we truncate the attacks such that $z_k = \bar{\delta}_k^T \bar{\delta}_k \leq \alpha$. This truncation to quantify the \bar{p} -probable ellipsoidal bound for the reachable set due to hidden attacks now imposes the same constraint that exists in the case of zero alarm attacks, see (10).

When we look at the complete reachable state of the system, we can decompose the contributions due to system noise and due to attack separately. Using the superposition principle of linear systems, the estimation error e_k can be written as $e_k = e_k^v + e_k^\delta$, where e_k^v denotes the part of e_k driven by noise and e_k^δ is the part driven by attacks. We can now write the estimation error dynamics in (14) as follows, where we assume the attack starts at $k = k^*$,

$$e_{k+1}^v = Fe_k^v + v_k, \quad e_{k^*}^v = e_{k^*} \quad (15)$$

$$e_{k+1}^\delta = Fe_k^\delta - L\Sigma^{\frac{1}{2}}\bar{\delta}_k, \quad e_{k^*}^\delta = \mathbf{0}. \quad (16)$$

Similarly, the state of the system x_k can be written as $x_k = x_k^v + x_k^\delta$, where x_k^v denotes the part of x_k driven by noise and x_k^δ is the part driven by attacks. Using this new notation, we can write the system dynamics in (12) as follows,

$$x_{k+1}^v = (F + GK)x_k^v - GKe_k^v + v_k, \quad x_{k^*}^v = x_{k^*} \quad (17)$$

$$x_{k+1}^\delta = (F + GK)x_k^\delta - GKe_k^\delta, \quad x_{k^*}^\delta = \mathbf{0}. \quad (18)$$

With these definitions, there are two reachable sets we aim to identify: the reachable states due to noise and due to attack. Because the state equation depends on the estimation error, in general, we must first identify the reachable estimation error due to noise and due to attack. Interestingly, the noise equations (15) and (17) have a special symmetry due to the zero initial conditions, i.e., $x_1^v = e_1^v = \mathbf{0}$. By writing

out e_k^v and x_k^v for each $k = 1, 2, \dots$, it quickly becomes clear that $x_k^v = e_k^v$ for all $k \in \mathbb{N}$. Thus, for the contribution driven by noise, we need only to solve the e_k^v equation. The reachable set of the estimation error driven by noise equals the reachable set of the states driven by noise.

Notice that the noise, a multivariate Gaussian distribution, also has unbounded support, thus it also has an infinite reachable set. We use the notion of a \bar{p} -probable reachable set to define a finite reachable set; for an equitable contribution by noise and attack, we again select $\bar{p} = 1 - \mathcal{A}$ and truncate the distribution with \bar{v} such that

$$\Pr(v_k^T R_1^{-1} v_k \leq \bar{v}) = \bar{p} = 1 - \mathcal{A}, \quad (19)$$

where R_1 is the covariance matrix of the system noise v_k . Since $v_k^T R_1^{-1} v_k$ is a chi-squared random variable with n degrees of freedom, the value of \bar{v} can be determined by Lemma 1. Thus for noises, $k \in \mathbb{N}$,

$$\mathcal{R}_e^v = \mathcal{R}_e^v = \{e_k^v \in \mathbb{R}^n \mid (15), v_k^T R_1^{-1} v_k \leq \bar{v}\}. \quad (20)$$

For attacks, $\forall k \geq k^*$,

$$\mathcal{R}_e^\delta = \{e_k^\delta \in \mathbb{R}^n \mid (16), \bar{\delta}_k^T \bar{\delta}_k \leq \alpha\}, \quad (21)$$

$$\mathcal{R}_x^\delta = \{x_k^\delta \in \mathbb{R}^n \mid (18), e_k^\delta \in \mathcal{R}_e^\delta\}. \quad (22)$$

A. LMI Approach

In general, it is analytically intractable to compute a reachable set \mathcal{R} exactly. Instead, using Linear Matrix Inequalities (LMIs), for some positive definite matrix \mathcal{P} , we derive *outer ellipsoidal bounds* of the form $\mathcal{E} = \{\xi_k \mid \xi_k^T \mathcal{P} \xi_k \leq 1\}$ containing \mathcal{R} . Our LMI results leverage the following lemma; this approach parallels work in [10], [15] however, the attack definitions are different, so they should be reformulated here.

Lemma 2: [16]. Let V_k be a positive definite function, $V_1 = 0$, and $\zeta_k^T \zeta_k \leq \kappa \in \mathbb{R}_{>0}$. If there exists a constant $a \in (0, 1)$ such that the condition below holds, then $V_k \leq 1$:

$$V_{k+1} - aV_k - \frac{1-a}{\kappa} \zeta_k^T \zeta_k \leq 0. \quad (23)$$

We present a generic solution to identify the outer bounding ellipsoids we need. We consider a linear system driven by an input that is elliptically bounded, which, as we will show, represent the dynamics in (15)-(18) and the corresponding constraints in (20)-(22).

Proposition 1: Given a LTI system $\xi_{k+1} = A\xi_k + B\mu_k$, $A \in \mathbb{R}^{n \times n}$ and $B \in \mathbb{R}^{n \times p}$, with the constraint $\mu_k^T R \mu_k \leq 1$, $R > 0$, for all $k \in \mathbb{N}$, if there exists $a \in (0, 1)$ and positive definite matrix $\mathcal{P} \in \mathbb{R}^{n \times n}$ that solves the convex optimization,

$$\begin{cases} \min_{\mathcal{P}} -\log \det \mathcal{P}, \\ \text{s.t. } \mathcal{P} > 0, \text{ and} \\ \begin{bmatrix} a\mathcal{P} - A^T \mathcal{P} A & -A^T \mathcal{P} B \\ -B^T \mathcal{P} A & (1-a)R - B^T \mathcal{P} B \end{bmatrix} \geq 0, \end{cases} \quad (24)$$

then the reachable states $\mathcal{R} \subseteq \mathcal{E} = \{\xi_k \in \mathbb{R}^n \mid \xi_k^T \mathcal{P} \xi_k \leq 1\}$ and the ellipsoid \mathcal{E} has minimum volume.

Proof: Let $V_k = \xi_k^T \mathcal{P} \xi_k$ and $\zeta_k = R^{\frac{1}{2}} \mu_k$ in (23) in Lemma 2, where $R^{\frac{1}{2}}$ is the symmetric square root of the

positive definite matrix R . It is easy to confirm that $\zeta_k^T \zeta_k = (R^{\frac{1}{2}} \mu)^T (R^{\frac{1}{2}} \mu) = \mu_k^T R \mu_k \leq 1$ with $\kappa = 1$. Substituting the dynamic equation for ξ_{k+1} in V_{k+1} yields an expression that when factored into quadratic form $\nu_k^T Q \nu_k \geq 0$, with $\nu_k = [\xi_k^T, \mu_k^T]^T$, the matrix Q is the LMI in the optimization problem above. Thus the bounding ellipsoid is given by $\mathcal{E} = \{\xi_k \mid V_k = \xi_k^T \mathcal{P} \xi_k \leq 1\}$.

To ensure that the ellipsoid bound is as tight as possible, we minimize $(\det \mathcal{P})^{-\frac{1}{2}}$ since this quantity is proportional to the volume of \mathcal{E} . We instead minimize $\log \det \mathcal{P}^{-1}$ as it shares the same minimizer and because for $\mathcal{P} > 0$ this objective is convex [17]. ■

We now use this generic result to outer bound the four reachable sets we need (I_n is the $n \times n$ identity matrix).

Theorem 1: The reachable sets

$$\mathcal{R}_e^v = \mathcal{R}_x^v, \mathcal{R}_e^\delta, \text{ and } \mathcal{R}_x^\delta,$$

are contained in the minimum volume ellipsoids

$$\mathcal{E}_e^v = \mathcal{E}_x^v, \mathcal{E}_e^\delta, \text{ and } \mathcal{E}_x^\delta,$$

respectively, characterized by the positive definite matrices

$$\mathcal{P}_e^v = \mathcal{P}_x^v, \mathcal{P}_e^\delta, \text{ and } \mathcal{P}_x^\delta,$$

respectively, which are the solutions to the convex optimization in Proposition 1 with the following choices of A , B , and R , respectively:

- $\mathcal{P}_e^v = \mathcal{P}_x^v$: $A = F$, $B = I_n$, $R = \frac{1}{v} R_1^{-1}$,
- \mathcal{P}_e^δ : $A = F$, $B = -L\Sigma^{\frac{1}{2}}$, $R = \frac{1}{\alpha} I_p$,
- \mathcal{P}_x^δ : $A = F + GK$, $B = -GK$, $R = \mathcal{P}_e^\delta$.

Proof: The proofs of each case are quite similar. We prove the case for \mathcal{P}_x^δ and the rest follow a same pattern. In (22), we identified that $e_k^\delta \in \mathcal{R}_e^\delta$. Instead we impose $e_k^\delta \in \mathcal{E}_e^\delta$. These sets are not equal, but since the ellipsoid contains the reachable set, this still satisfies the requirement of (22) - it does so with extra conservatism by also including estimation errors $e_k^\delta \in \mathcal{E}_e^\delta \setminus \mathcal{R}_e^\delta$.

Setting $A = F + GK$ is straightforward comparing (18) to Proposition 1. Define the input vector $\mu_k = e_k^\delta$ such that

$$\mu_k^T R \mu_k = \mu_k^T \mathcal{P}_e^\delta \mu_k \leq 1, \quad (25)$$

since $(e_k^\delta)^T \mathcal{P}_e^\delta e_k^\delta \leq 1$ by the definition of the ellipsoid \mathcal{E}_e^δ . With this definition of μ_k , the corresponding input matrix that satisfies (18) is $B = -GK$. ■

Having derived the set of reachable states due to noise and due to attack, both bounded by ellipsoids, we now compose these together to yield the total reachable set of states. The superposition of two ellipsoidal sets has been studied extensively and labeled the geometric (Minkowski) sum such that $\mathcal{E}_1 \oplus \mathcal{E}_2 = \{x + y \mid x \in \mathcal{E}_1, y \in \mathcal{E}_2\}$. The complete reachable set is then $\mathcal{E}_x = \mathcal{E}_x^v \oplus \mathcal{E}_x^\delta$. It is possible to compose another convex optimization and LMI to combine the ellipsoids [15], the geometric sum provides a tighter resulting ellipsoid. When these techniques are used to

design controller and estimator gains, optimization methods are preferred, but in this work we do not follow this line of inquiry.

B. Geometric Approach

A geometric approach to finding the ellipsoidal bounds for the reachable set of states comes from the observation that the equations in (15)-(18) contain inputs that are ellipsoidally bounded, i.e., $\frac{1}{v} v_k^T R_1^{-1} v_k \leq 1$ and $\frac{1}{\alpha} \bar{\delta}_k^T \bar{\delta}_k \leq 1$ (in fact these are spherically bounded). The geometric sum introduced above provides an operation that simultaneously computes all possible combinations between two geometric sets. For example, the dynamics for $k \in \mathbb{N}$,

$$\xi_{k+1} = A\xi_k + B\mu_k, \quad \xi_1 = \mathbf{0}, \quad \text{with } \mu_k^T R \mu_k \leq 1, \quad (26)$$

can be interpreted as an ellipsoidal update. For $k = 1$,

$$\xi_2 = A\xi_1 + B\mu_1. \quad (27)$$

The $\mu_1^T R \mu_1 \leq 1$ bound identifies that any possible value of μ_1 belongs to an ellipse $\mu_1 \in \{\mu \mid \mu^T R \mu \leq 1\}$. Many ellipsoid calculations are more concise when the ellipsoid is characterized by its *shape matrix*, Q , $\mathcal{E}(Q) = \{\mu \mid \mu^T Q^{-1} \mu \leq 1\}$. With this definition it is easy to express the linear transformation of an ellipse: if $\xi = M\mu$ and $\mu \in \mathcal{E}(Q)$, then $\xi \in \mathcal{E}(MQM^T)$ [18]. Thus in this example $\mu_1 \in \mathcal{E}(R^{-1})$ and $\xi_2 \in \mathcal{E}(BR^{-1}B^T)$. Continuing,

$$\xi_3 = A\xi_2 + B\mu_2, \quad (28)$$

where $\xi_2 \in \mathcal{E}(BR^{-1}B^T)$ and $\mu_2^T R \mu_2 \leq 1$. In this case $\xi_3 \in \mathcal{E}(ABR^{-1}B^T A^T) \oplus \mathcal{E}(BR^{-1}B^T)$, where \oplus represents the geometric sum. Although the geometric sum of two ellipsoids is not necessarily an ellipsoid, there are straightforward techniques to tightly fit an ellipsoid around the resulting shape (see [18]) so we will consider for the rest of this paper that the geometric sum of two ellipsoids is an ellipsoid.

We see now that all possible values that ξ_k can take on will belong to an ellipsoid, and one that is iteratively updated along the lines of the discussion above. Now we will specialize these observations to the context here to find \mathcal{E}_x . We take the same approach as in the LMI method by splitting the dynamics into a contribution driven by noise and a contribution driven by the attack, $\mathcal{E}_x = \mathcal{E}_x^v \oplus \mathcal{E}_x^\delta$.

Theorem 2: Given the estimation and state equations (15) and (17) for the system driven by noise, the ellipse \mathcal{E}_x^v contains all possible values of x_k^v , i.e., $\mathcal{R}_x^v \subseteq \mathcal{E}_x^v$, with

$$\mathcal{E}_x^v = \bigoplus_{k=0}^{\infty} \mathcal{E}(\bar{v} F^k R_1 (F^k)^T). \quad (29)$$

Proof: Recall for the contribution driven by noise we need only to solve the e_k^v equation (15). Expanding the recursive definition we can express e_N^v (x_N^v) in terms of all the past terms,

$$x_N^v = e_N^v = \sum_{k=1}^{N-1} F^{N-1-k} v_k. \quad (30)$$

Note that v_i and v_j are independent and equivalently bounded. Therefore, the terms of (30) have identical ellipsoids, $\mathcal{E}(\bar{v}R_1)$ transformed by different powers of F ,

$$\begin{aligned}\mathcal{E}_{x_N}^v &= \bigoplus_{k=1}^{N-1} \mathcal{E}(F^{N-1-k}(\bar{v}R_1)(F^{N-1-k})^T), \\ &= \bigoplus_{k=0}^{N-2} \mathcal{E}(\bar{v}F^k R_1 (F^k)^T).\end{aligned}\quad (31)$$

The ellipsoid that bounds all possible trajectories is the limiting ellipsoid as N goes to infinity. ■

Remark 2: We assume the matrix F is stable, otherwise the attacker can easily achieve arbitrarily large reachable sets simply by decoupling the controller from the open-loop system. Because of this, the volume of the ellipsoids (proportional to the determinant of their shape matrix) with higher powers of F become vanishingly small,

$$\det(\bar{v}F^k R_1 (F^k)^T) = \bar{v} \det(R_1) (\det F)^{2k}. \quad (32)$$

Since $\rho[F] < 1$, $\det F < 1$ and the volume goes to zero as k becomes large, so one can simply take N terms of the limiting geometric sum in (29) to achieve an accurate approximation of the bounding ellipsoid. The convergence of this sum (and hence the number of terms that should be chosen) depends on the spectrum of F .

Theorem 3: Given the estimation and state equations (16) and (18) for the system driven by attack, the ellipse \mathcal{E}_x^δ contains all possible values of x_k^δ , where,

$$\mathcal{E}_x^\delta = \bigoplus_{k=1}^{\infty} \mathcal{E}(\alpha H L \Sigma L^T H^T), \quad (33)$$

where $H = (F + GK)^k - F^k$. In other words $\mathcal{R}_x^\delta \subseteq \mathcal{E}_x^\delta$.

Proof: Expanding the recursive definitions in (18) and substituting in (16), we find

$$x_N^\delta = \sum_{k=1}^{N-2} ((F + GK)^{N-1-k} - F^{N-1-k}) L \Sigma^{\frac{1}{2}} \delta_k. \quad (34)$$

The rest of the proof follows the same line as the proof of Theorem 2 and so we omit the details. ■

Remark 3: Similarly, $\rho[F + GK] < 1$ because the controller matrix is selected to make the closed-loop system stable. Thus Theorem 3 benefits from the same practical advantage of constructing a good approximation of the ellipsoid \mathcal{E}_x^δ with finitely many terms.

IV. EMPIRICAL REACHABLE SETS

We now demonstrate these tools and provide a comparison between zero-alarm and hidden attacks. Although we generate a common bounding ellipsoid for both attacks, we also run extensive Monte-Carlo simulations to derive an approximation of the empirical reachable set the ellipsoids are meant to bound. We consider an LTI system (with matrices given underneath Table I) for this study with the

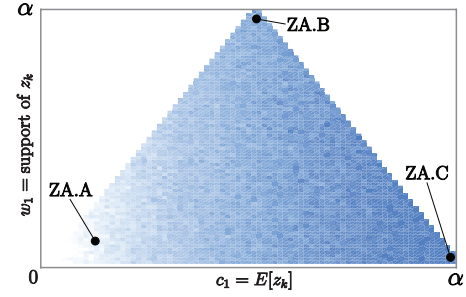


Fig. 3. The volume (blue is larger volume) of the reachable sets for different zero alarm z_k distributions of the form shown in Table I.

TABLE I
PARAMETERS FOR ZERO ALARM (ZA) AND HIDDEN (H) ATTACKS.

	ZA.A	ZA.B	ZA.C	H.A	H.B	H.C	H.D
c_1	$\alpha/8$	$\alpha/2$	α	α	α	α	α
w_1	$\alpha/10$	α	0	0	0	0	0
c_2	-	-	-	1.5α	2α	10α	100α
w_2	-	-	-	α	0	0	0

$$\begin{aligned}F &= \begin{bmatrix} 0.84 & 0.23 \\ -0.47 & 0.12 \end{bmatrix}, G = \begin{bmatrix} 0.07 & -0.32 \\ 0.23 & 0.58 \end{bmatrix}, C = \begin{bmatrix} 1 & 0 \\ 2 & 1 \end{bmatrix}, \\ R_1 &= \begin{bmatrix} 0.045 & -0.011 \\ -0.011 & 0.02 \end{bmatrix}, K = \begin{bmatrix} 1.404 & -1.042 \\ 1.842 & 1.008 \end{bmatrix}, \\ L &= \begin{bmatrix} 0.0276 & 0.0448 \\ -0.01998 & -0.0290 \end{bmatrix}, R_2 = \begin{bmatrix} 2 & 0 \\ 0 & 2 \end{bmatrix}, \Sigma = \begin{bmatrix} 2.086 & 0.134 \\ 0.134 & 2.230 \end{bmatrix}.\end{aligned}$$

chi-squared detector tuned to a false alarm rate $\mathcal{A} = 0.05$ (5%).

Fig. 1 clearly shows the ambiguity in designing zero alarm attacks and hidden attacks. In a zero alarm attack, the density function can be arbitrarily shaped on $z_k \leq \alpha$. For simplicity, consider that we use a uniform distribution of width w_1 and centered at $z_k = c_1$, such that the support of the distribution is over $[c_1 - \frac{w_1}{2}, c_1 + \frac{w_1}{2}]$. In other work, we have shown that in terms of steady-state deviation of the state, there exists a magnitude and “direction” of $\bar{\delta}_k$ that yields the strongest attack [13]. It is intuitive that maximizing the norm of the attack $\bar{\delta}_k^T \bar{\delta}_k = \alpha$ leads to stronger attacks than $\bar{\delta}_k^T \bar{\delta}_k < \alpha$. While we show an analytic result for the steady state deviation of the state [13], showing the same for the reachable sets is more nuanced. To demonstrate that this intuition holds empirically, we calculate the volume of the empirical reachable set attained through simulation. We approximate the volume by fitting an ellipsoid to the point cloud, where the lengths of the principle axes are given in terms of the eigenvalues of the data, as $1/\sqrt{\lambda_1}$ and $1/\sqrt{\lambda_2}$. The volumes are plotted in Fig. 3 for different choices of w_1 and c_1 and clearly shows the largest volume ellipsoids are generated by attacks for which $c_1 = \alpha$ and $w_1 \approx 0$. We select three sets of values for the pair (w_1, c_1) labeled ZA.A, ZA.B, and ZA.C for our comparison (see Table I).

For hidden attacks, there are two regions to define (below

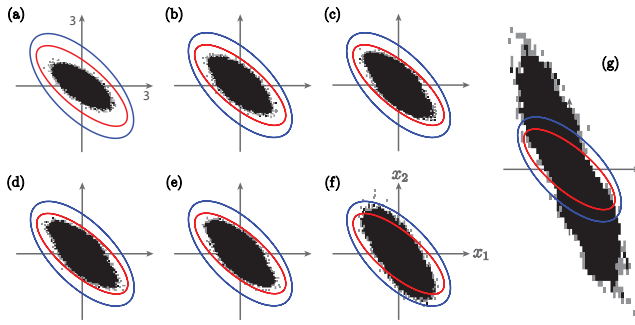


Fig. 4. The empirical reachable state sets in black with ellipsoidal bounds derived by the LMI approach (blue) and geometric approach (red) for zero alarm attacks (a) ZA.A, (b) ZA.B, and (c) ZA.C, as well as hidden attacks (d) H.A, (e) H.B, (f) H.C, and (g) H.D.

and beyond $z_k = \alpha$). Based on our prior observations (and intuition), we set the $1 - \mathcal{A}$ portion of the distribution that falls at or below α as a point mass at α . From Fig. 3, an attacker who wishes to maximize their influence on the reachable set would naturally make this choice. As discussed before, the second mass lies beyond α and could theoretically cause arbitrarily large reachable sets. Here we select the \mathcal{A} mass in four different configurations (parameterized by a second uniform distribution section centered at c_2 and with width w_2 , see Table I): spread uniformly from $(\alpha, 2\alpha]$ (labeled H.A), a point mass at 2α (H.B), a point mass at 10α (H.C), and a point mass at 100α (H.D).

In Fig. 4, we display the empirical reachable sets for all seven of these attacks as well as the LMI (blue) and geometric (red) outer ellipsoidal bounds derived with our methods. We first observe that both techniques are able to rather tightly bound the reachable set of states due to zero alarm attacks, although the geometric approach provides slightly tighter ellipsoid bounds. For hidden attacks, while it takes high magnitude attacked z_k values (e.g., $c_2 = 10\alpha$, 100α) to see a distinct growth in the volume of the reachable set, it is possible to grow the reachable set arbitrarily large.

The more substantial takeaway from this empirical study is that when we use conventional detectors that use a single cut in the distribution to determine if the current z_k is more likely to come from the original attack-free distribution or some other (attacked) distribution, we lack the ability to constrain the attacker due to the \mathcal{A} fraction of the distribution that falls beyond the detector threshold α . We require either a combination of detectors or modified definitions of current detectors to synthesize the information necessary to limit attackers further. When attackers hide in the infinite support of the noise, as in a hidden attack, we require some mechanism to effectively truncate or bound the impact of an attacker. Some obvious solutions are available, such as enforcing finite support of all noises, however, these approaches have not been integrated into conventional detector methods. In addition saying a disturbance as finite support is different from practically using this assumption; this gap must be addressed before this type of approach could be used.

V. CONCLUSION

We have presented a thorough exposition of the current ideology on using fault detection type detectors for identification of (sensor) attacks on control systems. In particular, we compared two attacks in which the opponent aims to remain stealthy - one in which the attack sequence is generated so as to not raise any alarms and one in which the attack sequence raises alarms at the same rate they occur in the absence of attacks. We developed two approaches to determine ellipsoidal and \bar{p} -probable ellipsoidal bounds (when the reachable set is infinite) on the reachable states of the system in response to the attack and to the inherent system noise. We demonstrated these concepts and methods with a numerical example that emphasizes the need for work that goes beyond traditional detectors.

REFERENCES

- [1] A. Cárdenas, S. Amin, Z. Lin, Y. Huang, C. Huang, and S. Sastry, "Attacks against process control systems: Risk assessment, detection, and response," in *Proceedings of the 6th ACM Symposium on Information, Computer and Communications Security*, 2011, pp. 355–366.
- [2] F. Pasqualetti, F. Dorfler, and F. Bullo, "Attack detection and identification in cyber-physical systems," *IEEE Transactions on Automatic Control*, vol. 58, pp. 2715–2729, 2013.
- [3] Y. Mo, E. Garone, A. Casavola, and B. Sinopoli, "False data injection attacks against state estimation in wireless sensor networks," in *Decision and Control (CDC), 2010 49th IEEE Conference on*, 2010, pp. 5967–5972.
- [4] C. Kwon, W. Liu, and I. Hwang, "Security analysis for cyber-physical systems against stealthy deception attacks," in *American Control Conference*, 2013, pp. 3344–3349.
- [5] F. Miao, Q. Zhu, M. Pajic, and G. J. Pappas, "Coding sensor outputs for injection attacks detection," in *Decision and Control (CDC), 2014 IEEE 53rd Annual Conference on*, 2014, pp. 5776–5781.
- [6] C. Z. Bai, F. Pasqualetti, and V. Gupta, "Security in stochastic control systems: Fundamental limitations and performance bounds," in *American Control Conference (ACC)*, 2015, pp. 195–200.
- [7] C. Murguia and J. Ruths, "Characterization of a cusum model-based sensor attack detector," in *proceedings of the 55th IEEE Conference on Decision and Control (CDC)*, 2016.
- [8] —, "Cusum and chi-squared attack detection of compromised sensors," in *proceedings of the IEEE Multi-Conference on Systems and Control (MSC)*, 2016.
- [9] Y. Mo and B. Sinopoli, "On the performance degradation of cyber-physical systems under stealthy integrity attacks," *IEEE Transactions on Automatic Control*, vol. 61, pp. 2618–2624, 2016.
- [10] C. Murguia, N. van de Wouw, and J. Ruths, "Reachable sets of hidden cps sensor attacks: Analysis and synthesis tools," in *proceedings of the IFAC World Congress*, 2016.
- [11] Y. Mo and B. Sinopoli, "Secure control against replay attacks," in *Communication, Control, and Computing, 2009. Allerton 2009. 47th Annual Allerton Conference on*, 2009, pp. 911–918.
- [12] K. J. Aström and B. Wittenmark, *Computer-controlled Systems (3rd Ed.)*. Upper Saddle River, NJ, USA: Prentice-Hall, Inc., 1997.
- [13] T. R. C. Murguia, and J. Ruths, "Tuning windowed chi-squared detectors for sensor attacks," in *American Control Conference*, 2018.
- [14] R. Langner, "Stuxnet: Dissecting a cyberwarfare weapon," *IEEE Security & Privacy*, vol. 9, no. 3, pp. 49–51, 2011.
- [15] C. Murguia and J. Ruths, "On reachable sets of hidden cps sensor attacks," in *American Control Conference*, 2018.
- [16] N. D. That, P. T. Nam, and Q. P. Ha, "Reachable set bounding for linear discrete-time systems with delays and bounded disturbances," *Journal of Optimization Theory and Applications*, vol. 157, pp. 96–107, 2013.
- [17] S. Boyd, L. El Ghaoui, E. Feron, and V. Balakrishnan, *Linear Matrix Inequalities in System and Control Theory*, ser. Studies in Applied Mathematics. Philadelphia, PA: SIAM, 1994, vol. 15.
- [18] A. A. Kurzhanskiy and P. Varaiya, "Ellipsoidal toolbox (et)," in *Decision and Control, 2006 45th IEEE Conference on*. IEEE, 2006, pp. 1498–1503.